Shoreface erosion counters blue carbon accumulation in transgressive barrier-island systems

Mary Bryan Barksdale[1,*], Christopher J. Hein[1], Matthew L. Kirwan[1]

[1]*Virginia Institute of Marine Science, William & Mary, P.O. Box 1346, Gloucester Point, VA 23062 USA*

* - corresponding author (mbarksdale@vims.edu)

Landward migration of coastal ecosystems in response to sea-level rise is altering coastal carbon dynamics. Although such landscapes rapidly accumulate soil carbon, barrier-island migration jeopardizes long-term storage through burial and exposure of organic-rich backbarrier deposits along the lower beach and shoreface. Here, we quantify the carbon flux associated with the seaside erosion of backbarrier lagoon and peat deposits along the Virginia Atlantic Coast. Barrier transgression leads to the release of approximately 26.1 Gg of organic carbon annually. Recent (1994–2017 C.E.) erosion rates exceed annual soil carbon accumulation rates (1984–2020) in adjacent backbarrier ecosystems by approximately 30%. Additionally, shoreface erosion of thick lagoon sediments accounts for >80% of total carbon losses, despite containing lower carbon densities than overlying salt marsh peat. Together, these results emphasize the impermanence of carbon stored in coastal environments and suggest that existing landscape-scale carbon budgets may overstate the magnitude of the coastal carbon sink.

The coastal landscape is widely recognized for its ability to store organic matter in "blue carbon" ecosystems, such as salt marshes and seagrass beds that bury carbon (C) in soils and sediments at rates orders of magnitude greater than terrestrial systems[1]. Sea-level rise (SLR) is thought to augment the coastal C sink[2], especially in marshes that are building soils vertically at rates similar to those of relative SLR[3–5]. A direct coupling between SLR and soil C accumulation can result in increases in C stocks even where marshes are eroding[2,6]. However, the capacity of the coastal zone to store blue carbon over centuries to millennia under rapid rates of SLR remains uncertain. For example, rapid SLR can exacerbate inundation stress and eventually lead to drowning of intertidal blue carbon coastal ecosystems, thereby reducing sequestration

33 potential while also degrading soil C[7–9]. Additionally, SLR can lead to large C losses within the
34 coastal zone by driving ecosystem transgression (for example, forest retreat, which prompts
35 substantial aboveground biomass loss[10,11] and/or by driving erosion of C-rich sediments when
36 exposed along open-ocean coasts[12,13]). Thus, coastal landscapes facing the combined threats of
37 SLR and erosion risk a blue carbon stock that is both diminished and more fleeting.
38 Barrier-island beach and dune systems protect the C-rich sediments of backbarrier marsh
39 from wave erosion along many coasts globally and can supply sediments to fringing backbarrier
40 marsh during high-energy events[14–16], processes that support lateral and vertical resilience to
41 SLR, respectively. However, this supportive function of barrier islands is jeopardized by SLR,
42 which, compounded with intensifying coastal storms and sediment deprivation, forces oceanside
43 barrier shorelines to transgress (through island narrowing via erosion and/or wholesale landward
44 migration) at accelerating rates[17,18]. Soil C stocks previously protected by barrier islands are
45 eventually exposed and subjected to high-energy, open-ocean processes, possibly shifting
46 transgressive barrier-island systems from C sinks to C sources[12].
47 Across the coastal landscape, the magnitude of the net C sink depends on the balance[19]
48 between C loss due to erosion or drowning, and C accumulation in ecosystems migrating and/or
49 accreting apace with SLR[2,6,11,20]. However, these landscape-scale C budgets typically focus on
50 the evolution only of vegetated ecosystems, and assume shallow depths of erosion, as is common
51 in protected environments. In contrast, wave action along open-ocean shorefaces can rework
52 sediments well below mean sea level, exposing to erosion not only surficial salt marsh peat, but
53 also far deeper sedimentary deposits. Failure to account for these processes may lead to large
54 overestimates of C storage in coastal ecosystems.

Here, we combine geospatial data of barrier island retreat rates, organic carbon (OC) accumulation rates within backbarrier marsh soils and seagrass and lagoon sediments, and the OC content of eroding sedimentary facies to develop a regional-scale OC budget for the rapidly transgressing Virginia Atlantic coast (USA). Sedimentologic and geochemical analyses of 10 new sediment cores (each 3–19 m long) together with additional published stratigraphic data were used to determine facies-specific thicknesses, OC densities, and OC erosion rates (Fig. 1; equation 1). We find that buried lagoon sediments associated with unvegetated environments contribute the vast majority (> 80%) of OC eroded on the beach and shoreface of transgressing barrier islands. Moreover, we find that erosion of these deep deposits leads to rates of OC loss that exceed annual OC accumulation summed across the entire backbarrier environment, despite the well-known capacity of blue carbon ecosystems to sequester OC.

Barrier island stratigraphy and carbon characteristics

The largely undeveloped and rapidly transgressing Virginia Barrier Islands (VBI) are located in the mid-Atlantic SLR hotspot[21] and generally characterized by either wholesale landward migration or rotation of formerly progradational islands[22] (Fig. 1a). Stratigraphic and OC analyses reveal that those islands which are migrating landward are characterized by thin (< 2 m thick) sandy beach and dune deposits[22] perched atop discontinuous, thin (~0.9 m) marsh peat and thick (~6.6 m) lagoon deposits (Fig. 1c). In contrast, former backbarrier peats associated with historically progradational islands (Parramore, Hog) were long-ago eroded as those islands migrated to their landward-most positions, leaving only thinner (0.75–6.25 m) remnant lagoon deposits preserved under relatively thick (~4.5 m) barrier sands[22]. Averaged across the seven migrating islands, the beachface-exposed marsh is 0.9 m thick (ranging from 0.6 [Smith] to 1.3 m [Assawoman]) and characterized by a relatively homogenous mixture of marsh roots and silt-

78 or clay-dominant minerogenic sediment with an average OC density of 26.8 kg OC m^{-3} (ranging
79 from 23.3 [Smith] to 31.5 kg OC m^{-3} [Cobb]; Fig. 1c; Table 1). In contrast, lagoon deposits
80 consist of a complex set of facies ranging from clay to medium sand, predominantly very dark
81 greenish grey in color, with frequent shell fragments. Across all ten islands, average lagoon
82 deposit thickness is 6.0 m (varying between 3.5 [Parramore] to 8.5 m [Wreck]) and average
83 lagoon OC density is 7.6 kg OC m^{-3} (ranging from 5.3 [Smith] to 10.1 kg OC m^{-3} [Cobb]; Fig.
84 1c). Sandy units interbedded within lagoon complexes average 0.8 m of very fine to very coarse
85 sand (ranging from 0.0 [Assawoman, Cobb, Myrtle] to 1.6 m [Metompkin and Cedar]). We
86 estimate that 38.8 km^2 of backbarrier marsh was buried and re-exposed by island migration along
87 the island chain from northern Assawoman to southern Smith between 1870 and 2017 C.E., at a
88 system-wide rate averaging 0.26 km^2 per year.
89 Although marsh peat is widely recognized for its large blue carbon stores[1], we find that
90 lagoon facies thickness is the single largest driver of shoreline-normalized OC erosion rates
91 (equation [1]), accounting for 85% of variability ($P < 0.001$; Fig. 2a). Shoreline-change rate
92 accounts for approximately half of the variability in OC erosion rates ($R^2 = 0.52$; $P = 0.02$; Fig.
93 2b). In contrast, neither the rate of long-term average marsh exposure ($P = 0.14$; Fig. 2c) nor
94 marsh or lagoon OC densities (Supplementary Fig. 1) have a significant effect on OC erosion
95 rates.
96 Applying new multi-decadal and island-specific shoreline-change rates, marsh-exposure
97 rates, and island shoreline lengths to equation (1) (Supplementary Tables 1–3), we find that
98 beach/shoreface OC erosion has accelerated over shorter time periods (Fig. 3), reaching an
99 annual average rate of 42.9 ± 10.0 Gg OC yr^{-1} between 1994 and 2017. This is more than 125%
100 greater than the average annual OC accumulation for the entire VBI backbarrier—including OC

accumulated in marsh, seagrass, and lagoon soil/sediment—over a similar time period (33.8 ± 6.0 Gg OC yr^{-1};1984–2020 C.E.)[23–25] (Fig. 3; Supplementary Table 4).

Implications for coastal carbon budgets

Carbon budgets that cross traditional ecosystem boundaries are crucial for establishing the degree to which coastal landscapes can mitigate climate change through C sequestration[11]. Recent studies demonstrate that ecosystem transitions associated with SLR (for example, conversion of forest to marsh or of marsh to open water) lead to shifts in magnitudes and loci of C burial and C loss[2,6,11,20]. However, such landscape-scale C budgets typically focus on vegetated ecosystems and include C loss due to marsh submergence or erosion only to a depth of 1 m[20,26,27]. Thus, widely-used protocols for assessing vulnerability of C stocks often overlook sediment C accumulation in unvegetated systems as well as C loss due to deeper erosion of non-vegetated facies. Here, by extending the landscape C budget to include sites of sediment/soil OC accumulation and erosion that traditionally have been ignored, we find that backbarrier lagoon and tidal-flat sediments contribute >80% of the total annual OC eroded in the VBI system (Fig. 3). Thus, incorporating these sediments into OC flux estimates not only magnifies the OC erosion term in our budget but also challenges previous understandings of the role deep, unvegetated sediments play in the coastal OC sink.

Organic C capture in vegetated ecosystems has been the paradigm of coastal OC research since the term 'blue carbon' was first coined in the early 2000s[1,7,28]. However, emerging evidence demonstrates that non-vegetated and subtidal coastal environments can contain substantial OC stocks[29,30], fed by the deposition of particulate matter (for example, organic matter from nearby erosion of vegetated systems or from productivity within the overlying water column) and *in situ* microphytobenthic productivity[31,32], as has been shown for the VBI

lagoons[33]. We find that, despite hosting OC densities that are approximately one-third of that of the marsh (Fig. 1c), the thickness of lagoon deposits is a more important driver of OC erosion fluxes than factors that commonly garner more attention, such as marsh OC density, marsh thickness, or marsh erosion rate (Figs. 2a and 2c; Supplementary Fig. 1). This aligns with emerging evidence that unvegetated coastal areas are important components of the coastal OC budget, and can, depending on their areal extent and thickness, account for more total OC storage than vegetated areas within the same landscape. In fact, we find that just the average annual erosion of lagoon OC (33.4 ± 9.8 Gg OC yr^{-1}; 1994–2017 C.E. could negate the OC accumulated annually in the entire backbarrier averaged over a similar time period (33.8 ± 6.0 Gg OC yr^{-1}; 1984–2020 C.E.) (Fig. 3).

The disproportionately high rates of OC burial in coastal ecosystems[1] leave large pools of OC subject to destabilization following rapid SLR and commensurate wetland drowning, forest dieback, and/or enhanced erosion[2,7,10]. Previous work by ref. [12] considered an additional consequence of SLR on OC storage (that is, transgression of barrier islands) and found that erosion of outcropping salt marsh along barrier-island beach and shorefaces can flip the system from a C sink to a C source. Likewise, our quantification of the most recent (1994–2017 C.E.) rate of annual OC erosion along the VBI shoreface is approximately 1.3 times the rate of OC accumulation across the entire VBI backbarrier over a similar time period[23–25] (Fig. 3; Supplementary Table 4). Including only marsh soil OC in these budgets would erroneously suggest that the VBI remains a strong sink for OC, netting an average 11.5 Gg OC yr^{-1} over the past two decades (Fig. 3; Supplementary Information). Like other landscape-scale carbon budgets[6,12,20,23], our work assumes that eroded carbon represents a source of carbon to the atmosphere or to non-coastal ecosystems. However, fully classifying the VBI chain as a net OC

147 source would require tracking the fate of this shoreface-eroded OC, which may include
148 remineralization, offshore burial, or possibly transport and redistribution to the backbarrier
149 through tidal inlets. Nevertheless, the imbalance we measure between annual rates of backbarrier
150 OC accumulation and shoreface OC erosion implies that, at the very least, barrier-island
151 transgression results in a coastal OC sink that is far more tenuous than commonly assumed.

152 **Blue carbon – climate feedbacks**

153 Blue C storage dynamics have traditionally been considered a negative climate feedback,
154 whereby SLR drives enhanced soil OC accumulation in coastal ecosystems like salt marshes[2–
155 4,6,9,34]. For the VBI, we find that an increase in the rate of island transgression by only 1 m yr^{-1}
156 intensifies OC erosion by approximately 73 kg OC m^{-1} yr^{-1} (Fig. 2b). Thus, our results
157 confuscate the current understanding of coastal OC processes by suggesting that dynamics along
158 open-ocean coasts can constitute a positive climate feedback. Given newly uncovered multi-
159 decadal lags in barrier response to SLR[18], our findings suggest that OC erosion along migrating
160 barrier islands will continue to accelerate as island movement equilibrates to modern (and even
161 faster, future) rates of SLR. Narrowly focusing on OC gains and losses within the top meter of
162 vegetated environments underestimates the OC potentially eroded from deeper and unvegetated
163 ecosystems, especially within dynamic coastal systems. Therefore, landscape-scale OC budgets
164 based on the evolution of shallow, vegetated environments may obscure the potential for coastal
165 landscapes to switch from net C sinks to C sources, a threshold which the VBI may already have
166 crossed. Regardless of the magnitudes and sites of OC accumulation and erosion, our findings
167 demonstrate that, for systems in which barrier islands are free to move landward, blue carbon
168 stored in wetland and thick lagoon sediments is largely ephemeral.
169

Methods

Shoreline behavior

The Virginia Barrier Islands (VBI) comprise a 110-km-long chain of 12 mixed-energy islands backed by salt marsh and shallow lagoons along the US Mid-Atlantic Coast (Fig. 1a). The absence of artificial shoreline stabilization along all but Wallops Island allows most to erode and/or migrate landward in response to storms and SLR, which they do at an average rate of 4.35 m yr^{-1} (1851–2017)[18]. Excluding net-progradational Fisherman's Island (located at the southern longshore depocenter at the mouth of Chesapeake Bay), individual island shorelines transgress at rates between 3.1 m yr^{-1} (Cobb) and 7.5 m yr^{-1} (Ship Shoal)[18] (Fig. 1a). This process exposes expansive marsh deposits along the seaward side of many of these islands (Fig. 1b) and, visible at very low tide, lagoon deposits along the marsh periphery or directly under barrier sands.

Sediment Core Analyses

Nine vibracores (each 3–9 m long) and one GeoProbe core (19 m long) collected from across seven islands (Fig. 1a) were analyzed for organic-matter (OM) content via loss-on-ignition (LOI) and grain size, and a subset for total organic carbon (TOC) content (Supplementary Information). We apply the resulting marsh- and lagoon-specific conversion factors (Supplementary Fig. 2) to approximate OC content based on OM values for all downcore samples.

OC Erosion Rate Calculations

Contact between the marsh and lagoon unit, as well as the base of the Holocene barrier-system were determined according to sediment texture, mineralogy, and OM content, in keeping with the unit descriptions of ref. [35,36]. We estimated OC erosion rates (g OC yr^{-1}) associated with loss of both marsh and lagoon deposits for each island as:

$$OC\ erosion\ rate = (T_{marsh} * ER_{marsh} * \rho OC_{marsh}) + (T_{lagoon} * L_{shoreline} * SCR * \rho OC_{lagoon}) \quad \text{(equation 1)},$$

where, following ref. [12], we apply island-average OC densities, ρ_{OCx} (g OC m^{-3}), to the island-average thicknesses, T_x (m), of the marsh and lagoon units based on new and published cores[35,37–40] (Fig. 1c; Table 1; Supplementary Table 5). Unlike ref. [12], however, we account for lagoon sediment OC in our erosion terms, quantifying a maximum blue carbon loss term for erosion of the entire Holocene unit. Except where replaced by inlet fills, lagoon deposits ubiquitously underlie both transgressive and progradational islands within the VBI chain[35,36,39,41]. Thus, lagoon sediment volume loss is approximated by multiplying the shoreline length, $L_{shoreline}$ (m) (Supplementary Table 1), by the island-specific shoreline-change rate, *SCR* (m yr^{-1}) (Supplementary Table 2). In contrast, beach/shoreface marsh erosion is confined to discontinuous portions of migrating islands. Following ref. [42], we used the earliest-mapped backbarrier marsh extent and overlaid successive island positions up to 2017 C.E. to calculate a time-averaged annual marsh exposure rate due to island transgression, ER_{marsh} (m^2 yr^{-1}) (Supplementary Table 3). We used Digital Shoreline Analysis System (DSAS)[43] to calculate shoreline positions at 50-m spaced transects along the length of the VBI to calculate both long-term (1870–2017) and short-term (1870–1942; 1942–1994; 1994–2017) shoreline-change rates, *SCR.* System-wide rates are valued as the sum of component islands.

Acknowledgements

This work was supported by National Science Foundation Geomorphology and Land Use Dynamics Program (EAR-2022987) (CJH), and the National Science Foundation CAREER, LTER, and CZN programs (EAR-1654374, DEB-1832221, and EAR-2012670) (MLK). We thank S. Fate, J. Lewis, C. Clarke, J. Garber, E. Hein, K. Holcomb, N. Ingle, T. Meredith, T. Messerschmidt, G. Molino, and C. Obara for assistance collecting cores as well as J. Connell, K. Cahoon, A. Gravgaard, and G. Weeks for assistance in core collection and processing. We thank K. Holcomb, A. Wilke, S. Bates, and S. Miller for assistance accessing field sites and would like to thank all past and current stewards of the VBI lands and waters.

Author Contributions

C.J.H. and M.L.K. conceptualized the study. M.B.B. and C.J.H. conducted fieldwork. M.B.B. conducted all labwork, analyzed data, and wrote initial manuscript. All three interpreted results and contributed to manuscript writing and editing.

Competing Interests

The authors declare no competing interests.

Inclusion and Ethics Statement

Access to all sites was granted through partnership with The Nature Conservancy and U.S. Fish and Wildlife Service staff, who are acknowledged above. Research is considered locally relevant for the Eastern Shore of Virginia based on the need for accurate coastal carbon budgets and attendant ecosystem conservation efforts.

Data Availability

All data relating to short-term OC erosion rates, OM-to-TOC conversions, sediment core descriptions, and sediment core OC calculations have been deposited in the EDI Data Repository (DOI: https://doi.org/10.6073/pasta/4fa27832835a95630533bcb5464debe7) (ref. 44).

References

1. Mcleod, E. *et al.* A blueprint for blue carbon: toward an improved understanding of the role of vegetated coastal habitats in sequestering CO2. *Front Ecol Environ* **9**, 552–560 (2011).
2. Valentine, K. *et al.* Climate-driven tradeoffs between landscape connectivity and the maintenance of the coastal carbon sink. *Nat Commun* **14**, 1137 (2023).
3. Rogers, K. *et al.* Wetland carbon storage controlled by millennial-scale variation in relative sea-level rise. *Nature* **567**, 91–95 (2019).
4. Wang, F., Lu, X., Sanders, C. J. & Tang, J. Tidal wetland resilience to sea level rise increases their carbon sequestration capacity in United States. *Nat Commun* **10**, 5434 (2019).
5. Weston, N. B. *et al.* Recent acceleration of wetland accretion and carbon accumulation along the U.S. East Coast. *Earth's Futur* **11**, (2023).
6. Herbert, E. R., Windham-Myers, L. & Kirwan, M. L. Sea-level rise enhances carbon accumulation in United States tidal wetlands. *One Earth* **4**, 425–433 (2021).
7. Pendleton, L. *et al.* Estimating global "blue carbon" emissions from conversion and degradation of vegetated coastal ecosystems. *Plos One* **7**, e43542 (2012).
8. McTigue, N. D., Walker, Q. A. & Currin, C. A. Refining estimates of greenhouse gas emissions from salt marsh "blue carbon" erosion and decomposition. *Frontiers Mar Sci* **8**, 661442 (2021).
9. Rogers, K., Kellway, J. & Saintilan, N. The present, past and future of blue carbon. *Camb. Prism.: Coast. Futur* **1**, 1–35 (2023) doi:10.1017/cft.2023.17.
10. Smith, A. J. & Kirwan, M. L. Sea level-driven marsh migration results in rapid net loss of carbon. *Geophys Res Lett* **48**, (2021).

11. Warnell, K., Olander, L. & Currin, C. Sea level rise drives carbon and habitat loss in the U.S. mid-Atlantic coastal zone. *PLOS Climate* **6**, (2022).
12. Theuerkauf, E. J. & Rodriguez, A. B. Placing barrier-island transgression in a blue-carbon context. *Earth's Futur* **5**, 789–810 (2017).
13. Hein, C. J. & Kirwan, M. L. Marine transgression in modern times. *Annual Review of Marine Science* **16**, (2024).
14. Rodriguez, A. B., Fegley, S. R., Ridge, J. T., VanDusen, B. M. & Anderson, N. Contribution of aeolian sand to backbarrier marsh sedimentation. *Estuar Coast Shelf Sci* **117**, 248–259 (2013).
15. Walters, D. C. & Kirwan, M. L. Optimal hurricane overwash thickness for maximizing marsh resilience to sea level rise. *Ecol Evol* **6**, 2948–2956 (2016).
16. Castagno, K. A., Ganju, N. K., Beck, M. W., Bowden, A. A. & Scyphers, S. B. How much marsh restoration is enough to deliver wave attenuation coastal protection benefits? *Frontiers Mar Sci* **8**, (2022).
17. Moore, L. J., List, J. H., Williams, S. J. & Stolper, D. Complexities in barrier island response to sea level rise: Insights from numerical model experiments, North Carolina Outer Banks. *J Geophys Res Earth Surf 2003 2012* **115**, (2010).
18. Mariotti, G. & Hein, C. J. Lag in response of coastal barrier-island retreat to sea-level rise. *Nature Geoscience* **15**, 633–638 (2022).
19. Chapin, F. S. *et al.* Reconciling carbon-cycle concepts, terminology, and methods. *Ecosystems* **9**, 1041–1050 (2006).
20. Baustian, M. M., Stagg, C. L., Perry, C. L., Moss, L. C. & Carruthers, T. J. B. Long-term carbon sinks in marsh soils of coastal Louisiana are at risk to wetland loss. *J Geophys Res Biogeosciences* **126**, (2021).
21. Sallenger, A. H., Doran, K. S. & Howd, P. A. Hotspot of accelerated sea-level rise on the Atlantic coast of North America. *Nat Clim Change* **2**, 884–888 (2012).
22. Robbins, M. G., Shawler, J. L. & Hein, C. J. Contribution of longshore sand exchanges to mesoscale barrier-island behavior: Insights from the Virginia Barrier Islands, U.S. East Coast. *Geomorphology* **403**, 108163 (2022).
23. Smith, A. J., Berg, P., Chen, Y., Doney, S., Ewers Lewis, C.J., Gedan, K., LaRoche, C., McGlathery, K., Pace, M., Zinnert, J., Kirwan, M.L., Compensatory mechanisms absorb regional carbon losses within a rapidly shifting coastal mosaic. *Ecosystems* 1–15 (2023) doi:10.1007/s10021-023-00877-7.
24. Hutchings, J. A. *et al.* Carbon deposition and burial in estuarine sediments of the contiguous United States. *Global Biogeochem Cy* **34**, (2020).
25. Nichols, M. M. Sediment accumulation rates and relative sea-level rise in lagoons. *Mar Geol* **88**, 201–219 (1989).
26. DeLaune, R. D. & White, J. R. Will coastal wetlands continue to sequester carbon in response to an increase in global sea level?: a case study of the rapidly subsiding Mississippi river deltaic plain. *Climatic Change* **110**, 297–314 (2012).
27. IPCC 2014, 2013 Supplement to the 2006 IPCC Guidelines for National Greenhouse Gas Inventories: Wetlands, Hiraishi, T., Krug, T., Tanabe, K., Srivastava, N., Baasansuren, J., Fukuda, M. and Troxler, T.G. (eds). (IPCC, 2014).
28. Macreadie, P. I., Hughes, A. R. & Kimbro, D. L. Loss of 'blue carbon' from coastal salt marshes following habitat disturbance. *Plos One* **8**, e69244 (2013).

29. Phang, V. X. H., Chou, L. M. & Friess, D. A. Ecosystem carbon stocks across a tropical intertidal habitat mosaic of mangrove forest, seagrass meadow, mudflat and sandbar. *Earth Surf. Process. Landf.* **40**, 1387–1400 (2015).
30. Lin, W., Wu, J. & Lin, H. Contribution of unvegetated tidal flats to coastal carbon flux. *Glob. Chang. Biol.* **26**, 3443–3454 (2020).
31. MacIntyre, H. L., Geider, R. J. & Miller, D. C. Microphytobenthos: The ecological role of the "secret garden" of unvegetated, shallow-water marine habitats. I. Distribution, abundance and primary production. *Estuaries* **19**, 186–201 (1996).
32. Duarte, C. M., Middelburg, J. J. & Caraco, N. Major role of marine vegetation on the oceanic carbon cycle. *Biogeosciences* **2**, 1–8 (2005).
33. Priestas, A. M., Mariotti, G., Leonardi, N. & Fagherazzi, S. Coupled wave energy and erosion dynamics along a salt marsh boundary, Hog Island Bay, Virginia, USA. *J Mar Sci Eng* **3**, 1041–1065 (2015).
34. Kirwan, M. L. & Mudd, S. M. Response of salt-marsh carbon accumulation to climate change. *Nature* **489**, 550–553 (2012).
35. Finkelstein, K. & Ferland, M. A. Back-barrier response to sea-level rise, Eastern Shore of Virginia. *The Society of Economic Paleontologists and Mineralogists* (1987).
36. Shawler, J. L. *et al.* Relative influence of antecedent topography and sea-level rise on barrier-island migration. *Sedimentology* **68**, 639–669 (2021).
37. Finkelstein, K. Backbarrier contributions to a littoral sand budget, Virginia Eastern Shore, USA. *Journal of Coastal Research* **2**, 33–42 (1986).
38. Shawler, J. L., Ciarletta, D. J., Lorenzo-Trueba, J. & Hein, C. J. Drowned foredune ridges as evidence of pre-historical barrier-island state changes between migration and progradation. *Coastal Sediments Proceedings* 158–171 (2019).
39. Raff, J. L. *et al.* Insights into barrier-island stability derived from transgressive/regressive state changes of Parramore Island, Virginia. *Mar Geol* **403**, 1–19 (2018).
40. Halsey, S. D. Late Quaternary geologic history and morphologic development of the barrier island system along the Delmarva Peninsula of the Mid-Atlantic Bight. (University of Delaware, 1978).
41. Hein, C. J. *et al.* Leveraging the interdependencies between barrier islands and backbarrier saltmarshes to enhance resilience to sea-level rise. *Frontiers Mar Sci* **8**, 721904 (2021).
42. Deaton, C. D., Hein, C. J. & Kirwan, M. L. Barrier island migration dominates ecogeomorphic feedbacks and drives salt marsh loss along the Virginia Atlantic Coast, USA. *Geology* **45**, 123–126 (2017).
43. Thieler, E.R., Himmelstoss, E.A., Zichichi, J.L., and Ergul, A. Digital Shoreline Analysis System (DSAS) version 4.0—An ArcGIS extension for calculating shoreline change: U.S. Geological Survey Open-File Report 2008-1278, http://woodshole.er.usgs.gov/project-pages/DSAS/version4/ (2008).
44. Barksdale, M.B., Hein, C.J, Kirwan, M.L. Erosion Rates, Soil Core Descriptions and Organic Matter on the Virginia Coast ver 2. Environmental Data Initiative. https://doi.org/10.6073/pasta/4fa27832835a95630533bcb5464debe7. (2023)

Table and Figures

Table 1. Variables Used to Calculate Long-Term (1870–2017) Organic Carbon (OC) Erosion Rates for the Virginia Barrier Islands

	Marsh			Lagoon				Combined
Island	Thickness (m)	Exposure rate (m^2 yr^{-1})	OC density (kg OC m^{-3})	Thickness (m)	Shoreline change rate (m yr^{-1})	1870 island length (m)	OC density (kg OC m^{-3})	OC erosion rate (Gg OC yr^{-1})
Assa.	1.26 ± 0.25	14243 ± 672	23.6 ± 3.3	5.63 ± 0.38	4.74 ± 0.68	6599 ± 16	8.2 ± 1.0	1.86 ± 0.31
Met.	0.66 ± 0.16	53135 ± 2508	26.8 ± 3.9	7.26 ± 3.06	7.67 ± 1.45	11442 ± 16	6.7 ± 0.8	5.21 ± 2.06
Cedar	1.07 ± 0.27	41734 ± 1970	27.6 ± 4.0	7.63 ± 3.38	6.68 ± 1.37	10687 ± 16	9.1 ± 1.2	6.18 ± 2.52
Parra.	0.90* ± 0.36*	161 ± 8	26.8* ± 4.1*	3.50 ± 2.75	5.94 ± 1.82	13000 ± 16	7.6* ± 1.0*	2.04 ± 1.74
Hog	0.90* ± 0.36*	3775 ± 178	26.8* ± 4.1*	3.50[†] ± 2.75[†]	3.10 ± 1.95	11288 ± 16	7.6* ± 1.0*	1.01 ± 0.94
Cobb	0.98 ± 0.36*	15909 ± 751	31.5 ± 4.4	4.55 ± 1.98*	3.03 ± 2.77	10256 ± 16	10.1 ± 1.3	1.92 ± 1.47
Wreck	1.18 ± 0.88	22004 ± 1039	27.1 ± 3.9	8.47 ± 2.82	5.72 ± 3.21	3934 ± 16	7.5 ± 0.9	2.13 ± 1.09
S.S.	0.90* ± 0.36*	12432 ± 587	26.8* ± 4.1*	6.63* ± 1.98*	8.07 ± 3.14	3405 ± 16	7.6* ± 1.0*	1.68 ± 0.71
Myrtle	0.60 ± 0.36*	15240 ± 719	27.5 ± 4.3	6.90 ± 1.98*	6.38 ± 2.35	3659 ± 16	5.9 ± 0.8	1.20 ± 0.49
Smith	0.56 ± 0.24	46484 ± 2194	23.3 ± 4.8	5.98[†] ± 0.29	5.63 ± 1.01	12633 ± 16	5.3 ± 0.7	2.87 ± 0.58
								Combined Virginia Barrier Islands = 26.12 ± 4.36

Note: Island abbreviations are: Assa.=Assawoman; Met.=Metompkin; Parra.=Parramore; S.S.=Ship Shoal. For more information on how uncertainties and standards of error were calculated, refer to Supplementary Information.

* Based on the average of all migrating Virginia Barrier Islands due to a lack of cores or due to a lack of multiple island-specific cores when calculating uncertainty values

[†] Based on Parramore averages

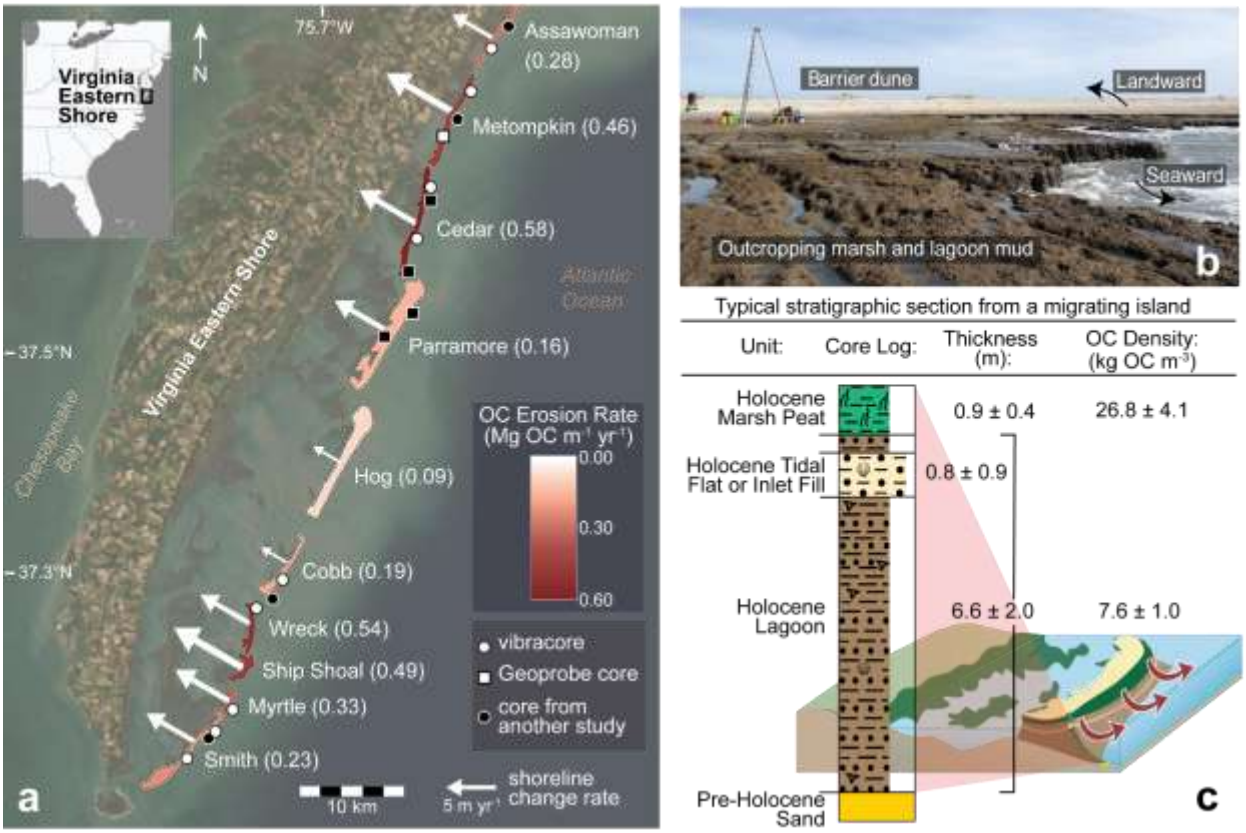

Figure 1. Shoreline changes, OC erosion rates, and beach and shoreface stratigraphy along the VBI. **a** The ten migrational and/or erosional/rotational Virginia Barrier Islands (Mid-Atlantic, USA). Island color and parenthetical values indicate organic carbon (OC) erosion rates, normalized by shoreline length. Length and width of white arrows correspond to long-term (1870–2017 C.E.) island-averaged shoreline change rates. **b** Ground view of backbarrier marsh and lagoon sediments exposure along the eroding beachface, and backed by a landward-migrating sandy beach and dune system. **c** Typical stratigraphic section from sediment cores penetrating through beachface-exposed marsh (as in b) along a landward-migrating island, noting stratigraphic units with associated average thicknesses and OC densities.

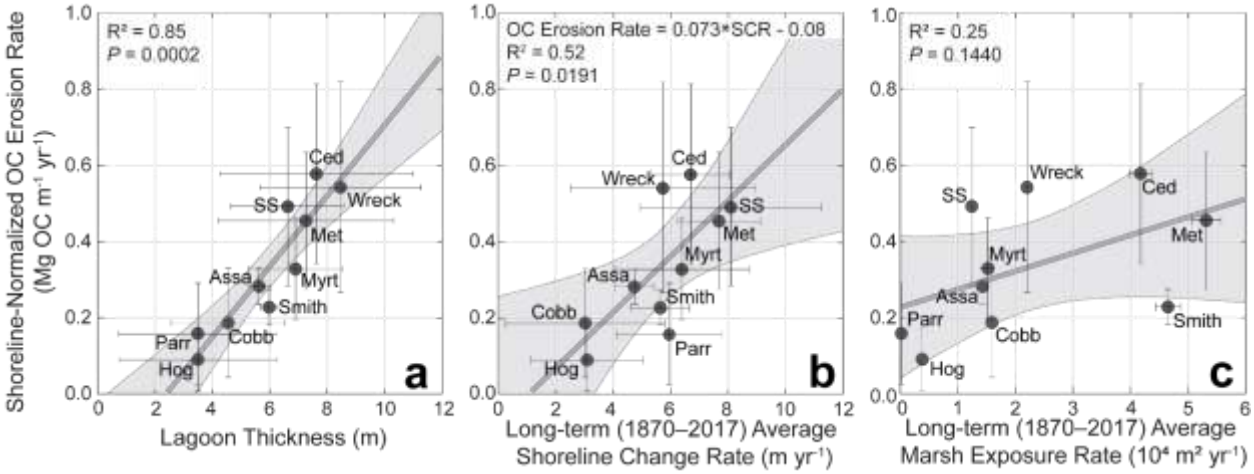

Figure 2. Drivers of OC erosion rates along the beach and shorefaces of the VBI. Comparisons between average annual organic-carbon (OC) erosion rates and drivers. Shown are regressions between shoreline-normalized OC erosion rates and **a** Lagoon thickness, **b** Long-term (1870–2017 C.E.) shoreline change rates, and **c** Long-term average marsh exposure rate. Solid lines indicate fitted linear regressions; gray windows demarcate 95% confidence intervals. Island abbreviations: Assa=Assawoman; Met=Metompkin; Ced=Cedar; Parr=Parramore; SS=Ship Shoal; Myrt=Myrtle.

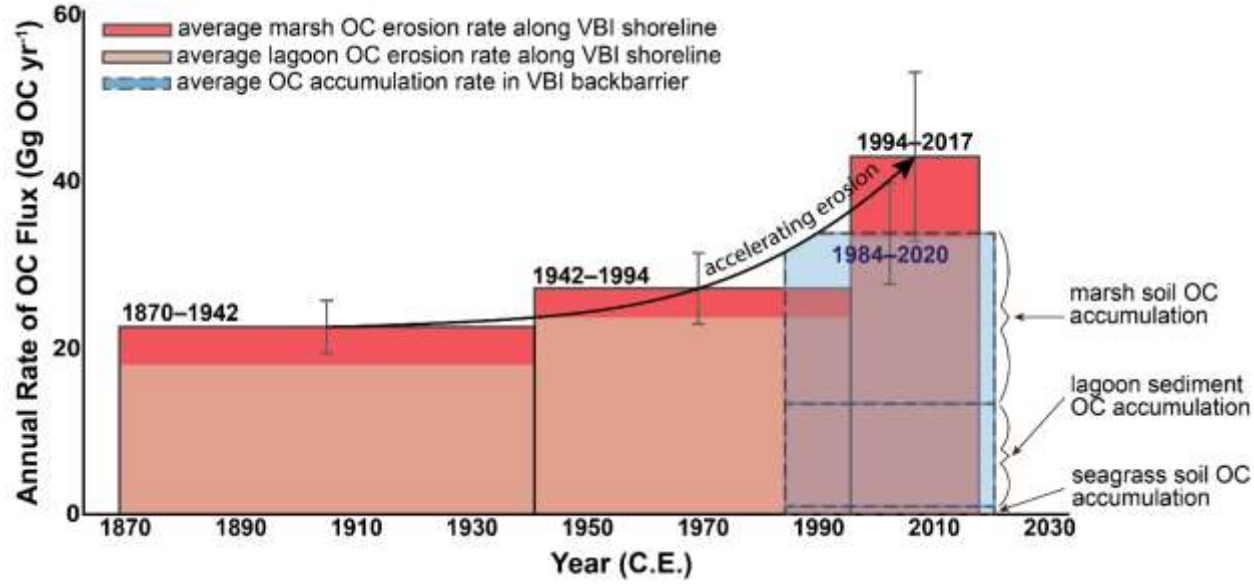

Figure 3. Multi-decadal OC erosion and accumulation rates for the VBI. Rates of annual organic carbon (OC) flux in the Virginia Barrier Islands (VBI) between 1870 and 2017 C.E. Gray bars represent uncertainty associated with each calculation.